JOURNAL OF AIRCRAFT
Vol. 36, No. 6, November–December 1999

Active Control of Structure-Borne and Airborne Sound Transmission Through Double Panel

Paolo Gardonio* and Stephen John Elliott†
University of Southampton, Highfield, Southampton SO17 1BJ, United Kingdom

This paper presents a theoretical study of the active control of both structure-borne and airborne noise transmission through a double-panel system. The physical and geometrical characteristics of the system were chosen to be similar to those of the fuselage of a civil aircraft. The total sound power transmitted by the double-panel system was used to evaluate the active control performance of four different strategies for the control system: first, active mounts connecting the two panels and loudspeakers placed between the two panels were driven to minimize the total sound power radiated by the panel (the reference case); second, active mounts connecting the two panels were driven to cancel the out-of-plane velocities at the connecting points on the radiating panel; third, loudspeakers placed between the two panels were driven to cancel the acoustic pressure at points near each control loudspeaker; and fourth, active mount and control loudspeaker systems were used simultaneously as already stated. The simulations show that the control loudspeakers are able to produce large attenuation of the sound transmission at low frequencies close to the mass-air-mass resonance of the double panel. The performance is significantly better if the loudspeakers are driven to minimize radiated sound power, rather than cancel pressure between the panels. The active mount configuration studied in this paper does not produce significant reductions of the sound transmission except in the case where it is used in combination with the control loudspeakers.

I. Introduction

INTERIOR cabin noise in civil aircraft has been studied widely in the past four decades, and it is now possible to find general reviews summarizing the most important aspects of the problem.[1–3] Several studies have been published on the classification of the main sources of interior noise,[4–12] on the identification of airborne and structure-borne noise transmission paths,[10–19] and on the evaluation of the effects produced by added passive treatments to reduce the noise transmission to the cabin.[20,21] This paper is focused on the problem of noise transmission through the fuselage of aircraft, which is defined as the airborne transmission path in the literature.[1] Many experiments on either laboratory test structures or real aircraft fuselage structures have shown that, in general, the sound-transmission reduction effects of stiffening, mass addition, and damping treatments of the fuselage skin vary with frequency and tend to be more effective at relatively high frequencies.[20,21] Good improvement in noise reduction is obtained when double-panel constructions with acoustic treatments (high-density fiberglass blankets) are used.[16,17,22–25] However, double-panel treatments provide good sound attenuation only at frequencies above the mass air mass resonance.[26] Grosveld[24] has shown that the blanket of absorbing material placed between the fuselage skin and the trim panel does not eliminate the mass-air-mass resonance.

Recent studies[27–32] have shown that improvements in the noise isolation at relatively low frequencies could be achieved using active control systems acting on the fuselage double-panel system. As shown in Fig. 1, in this paper two types of active control actuators are studied: first, an active mounting system that is used to attach the trim panel to the fuselage structure and second, a control loudspeaker system placed in the space between the trim panel and the skin of the fuselage. Three different configurations of the actuators have been investigated: first, only active mounts; second, only control loudspeakers; and third, both active mounts and control loudspeakers. The reduction in the total sound power radiation is estimated when using these three configurations of the control actuators. The reductions in the radiated sound power are also investigated when the active mounts are driven to cancel the out-of-plane velocities at the point where the mounts are connected to the receiver panel and when the control loudspeakers are driven to cancel the acoustic pressure at points between the panels, near to each control loudspeaker. The effect of using both active mounts and control loudspeakers in combination when velocities and acoustic pressure are cancelled is also investigated.

To study the effectiveness of these control systems, a theoretical model of sound transmission through a section of the fuselage double-wall system has been developed. In general, three different models of sound transmission through the fuselage of an aircraft could be used depending on the frequency range of the problem being considered.[1] At low frequencies, such that the longitudinal and circumferential wavelength of the fuselage skin flexural vibrations are longer than the stiffeners spacing (ring frames and stringers), the sound transmission into the cabin could be calculated using a smeared shell model.[33,34] This model calculates the sound transmission through the fuselage considered as an equivalent orthotropic cylindrical skin whose dynamics includes the mass and stiffness effects of the stiffeners. An alternative approach considers the noise transmission through a monocoque shell with rings and stiffeners treated as discrete structural elements.[35] For intermediate frequencies, up to 1 kHz, the vibrations of the frames become less important so that only the effects of the fuselage skin and longitudinal stringers need to be considered in the calculation of the noise transmission of a fuselage section between two adjacent frames.[36–38] For frequencies beyond 1 kHz (high frequencies), the dynamics of the stringers no longer affect the fuselage skin vibration.[1,28,37] To calculate the noise transmission, it is then necessary to consider only a section of the fuselage skin confined between two adjacent frames and two adjacent stringers. For the purposes of the study presented in this paper, a model has been chosen that is valid in the intermediate frequency region.

Most of the analytic studies of sound transmission through aircraft fuselage double walls assumes that the walls are acoustically coupled only and usually are flat.[39–44] The finite element method can be used to study a section of the fuselage double wall of finite size,[25] but the model can become complicated and physical insight limited. The results presented here have been obtained by using an

Received 2 May 1998; presented as Paper 98-2353 at the AIAA/CEAS 4th Aeroacoustics Conference, Tolouse, France, 2–4 June 1998; revision received 12 April 1999; accepted for publication 13 April 1999.

*Lecturer, Institute of Sound and Vibration Research.

†Professor of Adaptive Systems, Institute of Sound and Vibration Research.

approach where the system is divided into individual components[45]: the source panel, the transmitting system, and the receiving panel, and each component is studied in terms of point and transfer mobilities or impedances.[46]

Although some mechanisms of sound excitation, transmission, and radiation of the fuselage double wall of an aircraft have been neglected in this model, it is felt to contain the most important features of the problem and therefore should provide a good understanding of the phenomena occurring when active mounts or control loudspeakers are used.

II. Matrix Model

The mathematical model developed next assumes that the system is divided into three elements as shown in Fig. 2: the source panel (section of fuselage between two adjacent frames including a finite number of stringer stiffeners), the receiving panel (trim panel), and the structure-borne and airborne transmitting paths. (In this paper structure-borne path and airborne path are assumed to be the sound transmitted to the receiver trim panel via the frame-mounting system or via the medium confined between the trim panel and the fuselage skin, respectively.) The forces generated by active mounts fixed to the frames would produce local perturbations on the frames that would be transmitted to the fuselage skin. Because the model chosen does not account for the presence of the frames, these coupling effects have been modelled by structurally connecting the two panels thorough a set of small cylindrical rubber mounts. The panels are also fully acoustically coupled via the response of a small heavily damped enclosure. The dynamics of each of these elements is evaluated using point and transfer mobility or impedance terms. The three elements are modelled as distributed systems on which structural or acoustical waves can propagate. The acoustical coupling between the panels and the backpressure on the panels are calculated using the transfer impedances between a finite number of elements on the surface of the panels. The excitation of the source panel by an incident acoustic wave and the radiated sound power from the receiver panel are also calculated by assuming the two panels are divided up into a finite number of elements. Both the source and receiver panels are assumed to be baffled but otherwise in free space.

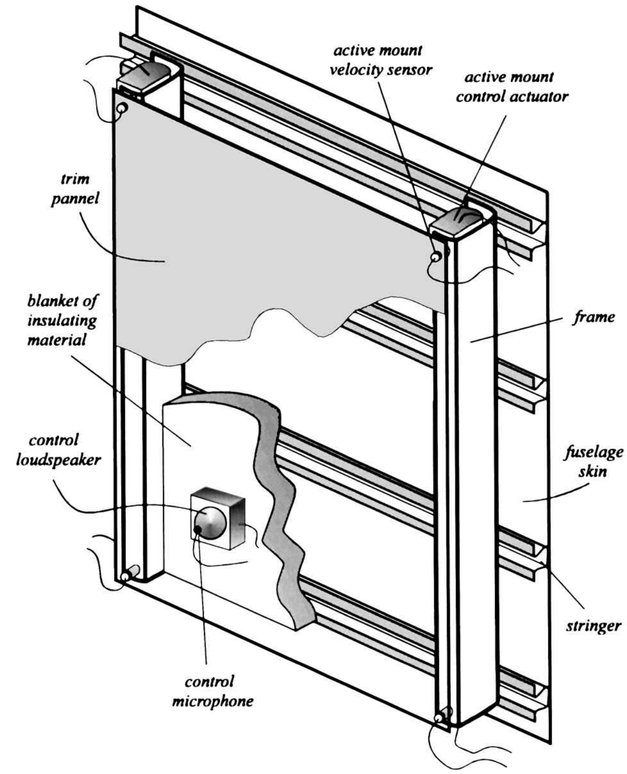

Fig. 1 Sketch of an aircraft fuselage section.

The structural path of the transmitting system consists of n distributed mounts. The mounts are connected to the source and receiver panels at a finite number of junctions. At each mount junction the motion and the forces transmitted are characterized by six complex parameters at a single frequency of excitation corresponding to six degrees of freedom. These velocity and force parameters are grouped into a velocity junction vector and a force junction vector, which, for the jth junction, can be written as

$$\boldsymbol{v}_{\mathrm{mj}} \equiv \{\dot{u}_j \quad \dot{v}_j \quad \dot{w}_j \quad \dot{\theta}_{xj} \quad \dot{\theta}_{yj} \quad \dot{\theta}_{zj}\}^T \tag{1}$$

$$\boldsymbol{f}_{\mathrm{mj}} \equiv \{N_{xj} \quad N_{yj} \quad N_{zj} \quad M_{xj} \quad M_{yj} \quad M_{zj}\}^T \tag{2}$$

where $\dot{u}_j$, $\dot{v}_j$, $\dot{w}_j$ are the linear velocities respectively along the x, y, and z directions; $\dot{\theta}_{xj}$, $\dot{\theta}_{yj}$, $\dot{\theta}_{zj}$ are the angular velocities referred respectively to the x, y, and z axis; N_{xj}, N_{yj}, N_{zj} are the forces in the x, y, and z directions; and finally M_{xj}, M_{yj}, M_{zj} are the moments referred respectively to the θ_{xj}, θ_{yj}, and θ_{zj} rotations. The transmitting system also includes the effect of the acoustic transmission through the cavity confined between the source panel and the receiver panel. As shown schematically in Fig. 2, the boundaries that the cavity has with the source panel and receiver panel surfaces are modelled by a discrete number of elements k whose dimensions are much smaller than an acoustic wavelength. The remaining boundaries, at the edges, are assumed to be rigid walls. Each of these elements can vibrate in one direction, which is orthogonal to the surface of the element itself and is connected either to the source panel or to the receiver panel at a finite number of points, whose position is defined by the geometrical center of the element. At the junction of each element, the motion and forces transmitted are characterized

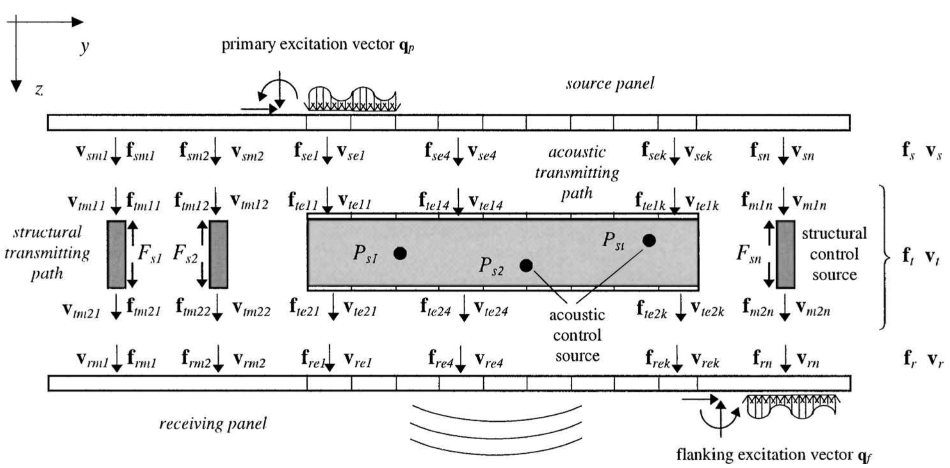

Fig. 2 Scheme of a general complete isolating system.

by only one complex parameter, at a single frequency of excitation, which can be written as

$$v_{ej} \equiv \dot{w}_j \qquad f_{ej} \equiv N_{zj} \tag{3, 4}$$

With reference to the notation shown in Fig. 2, combinations of these junction vectors are then grouped together to form three combined pairs of vectors: the source velocity vector $\boldsymbol{v}_s$ and force vector $\boldsymbol{f}_s$, the receiver velocity vector $\boldsymbol{v}_r$ and force vector $\mathbf{f}_r$, and the transmitting system velocity vector $\boldsymbol{v}_t$ and force vector $\boldsymbol{f}_t$. The source and receiver velocity vector and force vector are given by

$$\boldsymbol{v}_s \equiv \begin{Bmatrix} \boldsymbol{v}_{\mathrm{sm}} \\ \boldsymbol{v}_{\mathrm{se}} \end{Bmatrix} \equiv \begin{Bmatrix} \boldsymbol{v}_{\mathrm{sm1}} \\ \boldsymbol{v}_{\mathrm{sm2}} \\ \vdots \\ \boldsymbol{v}_{\mathrm{smn}} \\ v_{\mathrm{se1}} \\ v_{\mathrm{se2}} \\ \vdots \\ v_{\mathrm{sek}} \end{Bmatrix} \qquad \boldsymbol{f}_s \equiv \begin{Bmatrix} \boldsymbol{f}_{\mathrm{sm}} \\ \boldsymbol{f}_{\mathrm{se}} \end{Bmatrix} \equiv \begin{Bmatrix} \boldsymbol{f}_{\mathrm{sm1}} \\ \boldsymbol{f}_{\mathrm{sm2}} \\ \vdots \\ \boldsymbol{f}_{\mathrm{smn}} \\ f_{\mathrm{se1}} \\ f_{\mathrm{se2}} \\ \vdots \\ f_{\mathrm{sek}} \end{Bmatrix} \tag{5, 6}$$

$$\boldsymbol{v}_r \equiv \begin{Bmatrix} \boldsymbol{v}_{\mathrm{rm}} \\ \boldsymbol{v}_{\mathrm{re}} \end{Bmatrix} \equiv \begin{Bmatrix} \boldsymbol{v}_{\mathrm{rm1}} \\ \boldsymbol{v}_{\mathrm{rm2}} \\ \vdots \\ \boldsymbol{v}_{\mathrm{rmn}} \\ v_{\mathrm{re1}} \\ v_{\mathrm{re2}} \\ \vdots \\ v_{\mathrm{rek}} \end{Bmatrix} \qquad \boldsymbol{f}_r \equiv \begin{Bmatrix} \boldsymbol{f}_{\mathrm{rm}} \\ \boldsymbol{f}_{\mathrm{re}} \end{Bmatrix} \equiv \begin{Bmatrix} \boldsymbol{f}_{\mathrm{rm1}} \\ \boldsymbol{f}_{\mathrm{rm2}} \\ \vdots \\ \boldsymbol{f}_{\mathrm{rmn}} \\ f_{\mathrm{re1}} \\ f_{\mathrm{re2}} \\ \vdots \\ f_{\mathrm{rek}} \end{Bmatrix} \tag{7, 8}$$

where $\boldsymbol{v}_{\mathrm{smj}}$, $\boldsymbol{f}_{\mathrm{smj}}$ and $\boldsymbol{v}_{\mathrm{sej}}$, f_{sej} represent the velocities and forces at the source junction for the jth mount and for the jth acoustic element, while $\boldsymbol{v}_{\mathrm{rmj}}$, $\boldsymbol{f}_{\mathrm{rmj}}$ and $\boldsymbol{v}_{\mathrm{rej}}$, f_{rej} represent the velocities and forces at the receiver junction for the jth mount and for the jth acoustic element. The vectors of velocities and forces at each element of the transmitting system are given by

$$\boldsymbol{v}_t \equiv \begin{Bmatrix} \boldsymbol{v}_{\mathrm{tm1}} \\ \boldsymbol{v}_{\mathrm{te1}} \\ \boldsymbol{v}_{\mathrm{tm2}} \\ \boldsymbol{v}_{\mathrm{te2}} \end{Bmatrix} \equiv \begin{Bmatrix} \boldsymbol{v}_{\mathrm{tm11}} \\ \vdots \\ \boldsymbol{v}_{\mathrm{tm1}n} \\ v_{\mathrm{te11}} \\ \vdots \\ v_{\mathrm{te1}k} \\ \boldsymbol{v}_{\mathrm{tm21}} \\ \vdots \\ \boldsymbol{v}_{\mathrm{tm2}n} \\ v_{\mathrm{te21}} \\ \vdots \\ v_{\mathrm{te2}k} \end{Bmatrix} \qquad \boldsymbol{f}_t \equiv \begin{Bmatrix} \boldsymbol{f}_{\mathrm{tm1}} \\ \boldsymbol{f}_{\mathrm{te1}} \\ \boldsymbol{f}_{\mathrm{tm2}} \\ \boldsymbol{f}_{\mathrm{te2}} \end{Bmatrix} \equiv \begin{Bmatrix} \boldsymbol{f}_{\mathrm{tm11}} \\ \vdots \\ \boldsymbol{f}_{\mathrm{tm1}n} \\ f_{\mathrm{te11}} \\ \vdots \\ f_{\mathrm{te1}k} \\ \boldsymbol{f}_{\mathrm{tm21}} \\ \vdots \\ \boldsymbol{f}_{\mathrm{tm2}n} \\ f_{\mathrm{te21}} \\ \vdots \\ f_{\mathrm{te2}k} \end{Bmatrix} \tag{9, 10}$$

where $\boldsymbol{v}_{\mathrm{tm1}j}$, $\boldsymbol{f}_{\mathrm{tm1}j}$ and $v_{\mathrm{te1}j}$, $f_{\mathrm{te1}j}$ represent the velocities and forces at the source junction for the jth mount and for the jth acoustic element while $\boldsymbol{v}_{\mathrm{tm2}j}$, $\boldsymbol{f}_{\mathrm{tm2}j}$ and $v_{\mathrm{te2}j}$, $f_{\mathrm{te2}j}$ represent the velocities and forces at the receiver junction for the jth mount and for the jth acoustic element.

The dynamics of the source and receiver panels are modelled using a mobility matrix approach so that their velocity and force vectors can be written in the form:

$$\boldsymbol{v}_s = \boldsymbol{M}_{s1}\boldsymbol{f}_s + \boldsymbol{M}_{s2}\boldsymbol{q}_p \qquad \boldsymbol{v}_r = \boldsymbol{M}_{r1}\boldsymbol{f}_r + \boldsymbol{M}_{r2}\boldsymbol{q}_f \tag{11, 12}$$

where $\boldsymbol{M}_{s1}$, $\boldsymbol{M}_{s2}$ and $\boldsymbol{M}_{r1}$, $\boldsymbol{M}_{r2}$ are mobility matrices of the source and receiver panels and $\boldsymbol{q}_p$, $\boldsymbol{q}_f$ are the primary excitation vector and the flanking excitation vector. The flanking excitation acting on the receiver $\boldsymbol{q}_f$ could be caused by a subsystem connected to it or to an additional flanking path connecting the source panel to the receiver panel. A detailed description of the source and receiver panel mobility matrices is given in Ref 45. The dynamics of the transmitting system are expressed using an impedance matrix approach:

$$\boldsymbol{f}_t = \boldsymbol{Z}_{t1}\boldsymbol{v}_t + \boldsymbol{Z}_{t2}\boldsymbol{q}_s \tag{13}$$

where $\mathbf{Z}_{t1}$ and $\mathbf{Z}_{t2}$ are impedance matrices of the transmitting system[45] and $\boldsymbol{q}_s = \{\boldsymbol{q}_{\mathrm{sf}}\ \ \boldsymbol{q}_{\mathrm{sl}}\}^T$ is the excitation vector of the control forces acting on the mounts $\boldsymbol{q}_{\mathrm{sf}} = \{F_{s1}\ \ F_{s2}\ \ \cdots\ \ F_{\mathrm{sn}}\}$ and the source strength of the loudspeakers placed in the acoustic cavity $\boldsymbol{q}_{\mathrm{sl}} = \{P_{s1}\ \ P_{s2}\ \ \cdots\ \ P_{\mathrm{st}}\}$. Note that the components of the matrices $\boldsymbol{Z}_{t1}$ and $\boldsymbol{Z}_{t2}$ caused by the mounts are block diagonal, but those caused by the acoustic cavity are fully populated because a velocity at one element will generate a force caused by the pressure at all of the other elements. The source and receiver panel equations (11) and (12) can be grouped together in one equation:

$$\boldsymbol{v}_{\mathrm{sr}} = \boldsymbol{M}_{\mathrm{sr1}}\boldsymbol{f}_{\mathrm{sr}} + \boldsymbol{M}_{\mathrm{sr2}}\,\boldsymbol{q}_{\mathrm{pf}} \tag{14}$$

where the mobility matrices and the excitation vector have the form

$$\boldsymbol{M}_{\mathrm{sr1}} = \begin{bmatrix} \boldsymbol{M}_{s1} & 0 \\ 0 & \boldsymbol{M}_{r1} \end{bmatrix} \qquad \boldsymbol{M}_{\mathrm{sr2}} = \begin{bmatrix} \boldsymbol{M}_{s2} & 0 \\ 0 & \boldsymbol{M}_{r2} \end{bmatrix} \tag{15, 16}$$

$$\boldsymbol{q}_{\mathrm{pf}} = \begin{Bmatrix} \boldsymbol{q}_p \\ \boldsymbol{q}_f \end{Bmatrix} \tag{17}$$

and the junction velocity and force vectors are given by

$$\boldsymbol{v}_{\mathrm{sr}} \equiv \begin{Bmatrix} \boldsymbol{v}_s \\ \boldsymbol{v}_r \end{Bmatrix} \qquad \boldsymbol{f}_{\mathrm{sr}} \equiv \begin{Bmatrix} \boldsymbol{f}_s \\ \boldsymbol{f}_r \end{Bmatrix} \tag{18, 19}$$

where $\boldsymbol{v}_{\mathrm{sr}}$ and $\boldsymbol{f}_{\mathrm{sr}}$ are called respectively source-receiver velocity vector and source-receiver force vector. The source-receiver vectors are related to the analogous transmitting system vectors in such a way as to satisfy the continuity principle (for the velocity vectors) and the equilibrium principle (for the force vectors) at each junction:

$$\boldsymbol{f}_t + \boldsymbol{f}_{\mathrm{sr}} = 0 \qquad \boldsymbol{v}_t = \boldsymbol{v}_{\mathrm{sr}} \tag{20, 21}$$

Using these two relations, Eqs. (13) and (14) can be related in such a way as to find the vector of velocities of the elements on the source and receiver panel as a function of the primary-flanking and secondary sources:

$$\boldsymbol{v}_{\mathrm{sr}} = \boldsymbol{Q}_{\mathrm{pv}}\boldsymbol{q}_{\mathrm{pf}} + \boldsymbol{Q}_{\mathrm{sv}}\boldsymbol{q}_s \tag{22}$$

where

$$\boldsymbol{Q}_{\mathrm{pv}} = (\boldsymbol{I} + \boldsymbol{M}_{\mathrm{sr1}}\,\boldsymbol{Z}_{t1})^{-1}\boldsymbol{M}_{\mathrm{sr2}} \tag{23}$$

$$\boldsymbol{Q}_{\mathrm{sv}} = -(\boldsymbol{I} + \boldsymbol{M}_{\mathrm{sr1}}\,\boldsymbol{Z}_{t1})^{-1}\boldsymbol{M}_{\mathrm{sr1}}\,\boldsymbol{Z}_{t2} \tag{24}$$

The matrices $\boldsymbol{Q}_{\mathrm{pv}}$ and $\boldsymbol{Q}_{\mathrm{sv}}$ relate the behavior of the fully coupled system ($\boldsymbol{v}_{\mathrm{sr}}$, $\boldsymbol{f}_{\mathrm{sr}}$) to the primary-flanking and secondary excitations ($\boldsymbol{q}_{\mathrm{pf}}$, $\boldsymbol{q}_s$). The sound power radiated by the receiving panel can then be evaluated using the velocities of the radiating elements which are a subset of $\boldsymbol{v}_{\mathrm{sr}}$, as

$$W_r(\omega) = \boldsymbol{v}_{\mathrm{re}}^H \boldsymbol{R}\boldsymbol{v}_{\mathrm{re}} \tag{25}$$

where $\boldsymbol{R}$ is the radiation resistance matrix.[47]

III. Control Strategies

All of the strategies considered here for active control can be expressed in terms of a quadratic cost function, which is minimized and which can always be written in the form[48]

$$J = \boldsymbol{q}_s^H \boldsymbol{A} \boldsymbol{q}_s + \boldsymbol{q}_s^H \boldsymbol{b} + \boldsymbol{b}^H \boldsymbol{q}_s + c \tag{26}$$

The control source that minimizes this quadratic equation is given by[48]

$$\boldsymbol{q}_s(\mathrm{opt}) = -\boldsymbol{A}^{-1}\boldsymbol{b} \tag{27}$$

Four control strategies are studied: 1) minimizing total sound power radiation using either the active mounts or the control loudspeakers and using both the active mounts and the control loudspeakers; 2) cancellation of out-of-plane input velocities to the receiver using only active mounts; 3) cancellation of acoustic pressure at fixed points of the cavity using only control loudspeakers; and 4) cancellation of both out-of-plane input velocities to the receiver panel and acoustic pressure at fixed points of the cavity using both the active mounts and control loudspeakers.

In this paper these four control strategies will be referred to as 1) sound radiation minimization (J_{sr}), 2) velocity cancellation (J_v), 3) pressure cancellation (J_p), and 4) velocity and pressure cancellation ($J_{v,p}$). When the total sound radiation is minimized, the cost function is

$$J_{\mathrm{sr}} = \boldsymbol{v}_{\mathrm{re}}^H \boldsymbol{R} \boldsymbol{v}_{\mathrm{re}} \tag{28}$$

where the velocity vector $\boldsymbol{v}_{\mathrm{re}}$ contains only the velocities of the radiating elements on the receiver plate and is given by the following equation $\boldsymbol{v}_{\mathrm{re}} = \boldsymbol{S}_{\mathrm{re}}\boldsymbol{v}_{\mathrm{sr}}$. The two matrices required in the quadratic form of Eq. (26) are then:

$$\boldsymbol{A}_{\mathrm{sr}} = \boldsymbol{Q}_{\mathrm{sv}}^H \boldsymbol{S}_{\mathrm{re}}^T \boldsymbol{R} \boldsymbol{S}_{\mathrm{re}} \boldsymbol{Q}_{\mathrm{sv}} \qquad \boldsymbol{b}_{\mathrm{sr}} = \boldsymbol{Q}_{\mathrm{sv}}^H \boldsymbol{S}_{\mathrm{re}}^T \boldsymbol{R} \boldsymbol{S}_{\mathrm{re}} \boldsymbol{Q}_{\mathrm{pv}} \boldsymbol{q}_{\mathrm{pf}} \tag{29, 30}$$

When velocity cancellation is implemented, then the cost function has the form

$$J_v = \boldsymbol{v}_{\mathrm{rm}}^H \boldsymbol{v}_{\mathrm{rm}} \tag{31}$$

and the velocity vector $\boldsymbol{v}_{\mathrm{rm}}$, which contains only the out-of-plane velocity terms at the receiver panel junctions, is obtained with the following equation: $\boldsymbol{v}_{\mathrm{rm}} = \boldsymbol{S}_{\mathrm{rm}}\boldsymbol{v}_{\mathrm{sr}}$. The two matrices in Eq. (26) are then given by

$$\boldsymbol{A}_v = \boldsymbol{Q}_{\mathrm{sv}}^H \boldsymbol{S}_{\mathrm{rm}}^T \boldsymbol{S}_{\mathrm{rm}} \boldsymbol{Q}_{\mathrm{sv}} \qquad \boldsymbol{b}_v = \boldsymbol{Q}_{\mathrm{sv}}^H \boldsymbol{S}_{\mathrm{rm}}^T \boldsymbol{S}_{\mathrm{rm}} \boldsymbol{Q}_{\mathrm{pv}} \boldsymbol{q}_{\mathrm{pf}} \tag{32, 33}$$

When pressure cancellation is implemented, then the cost function has the form

$$J_p = \boldsymbol{p}_c^H \boldsymbol{p}_c \tag{34}$$

and the pressure vector $\boldsymbol{p}_c$ is given by $\boldsymbol{p}_c = \boldsymbol{Z}_{c1}\boldsymbol{v}_{\mathrm{sre}} + \boldsymbol{Z}_{c2}\boldsymbol{q}_{\mathrm{sl}}$. $\boldsymbol{Z}_{c1}$ and $\boldsymbol{Z}_{c2}$ are two matrices that give the pressure terms caused by the vibration of the boundary elements of the cavity $\boldsymbol{v}_{\mathrm{sre}} = \{\boldsymbol{v}_{\mathrm{se}}^T \;\; \boldsymbol{v}_{\mathrm{re}}^T\}^T$ taking into account both primary-flanking and secondary sources and caused by the direct field generated by the control loudspeaker source $\boldsymbol{q}_{\mathrm{sl}}$. In this case the velocities of the source and receiver boundary elements are given by $\boldsymbol{v}_{\mathrm{sre}} = \boldsymbol{S}_{\mathrm{sre}}\boldsymbol{v}_{\mathrm{sr}}$. The two matrices in Eq. (26) are then given by

$$\boldsymbol{A}_p = \left(\boldsymbol{P}_{2c}^H + \boldsymbol{Q}_{\mathrm{sv}}^H \boldsymbol{S}_{\mathrm{sre}}^H \boldsymbol{P}_{1c}^H\right)\left(\boldsymbol{P}_{1c}\boldsymbol{S}_{\mathrm{sre}}\boldsymbol{Q}_{\mathrm{sv}} + \boldsymbol{P}_{2c}\right) \tag{35}$$

$$\boldsymbol{b}_p = \left(\boldsymbol{P}_{2c}^H + \boldsymbol{Q}_{\mathrm{sv}}^H \boldsymbol{S}_{\mathrm{sre}}^H \boldsymbol{P}_{1c}^H\right)\boldsymbol{P}_{1c}\boldsymbol{S}_{\mathrm{sre}}\boldsymbol{Q}_{\mathrm{pv}}\boldsymbol{q}_{\mathrm{pf}} \tag{36}$$

Finally, when velocity and pressure minimization are implemented, then the cost function has the form

$$J_{v,p} = \left\{\boldsymbol{v}_{\mathrm{rm}}^H \;\; \boldsymbol{p}_c^H\right\}\begin{Bmatrix}\boldsymbol{v}_{\mathrm{rm}} \\ \boldsymbol{p}_c\end{Bmatrix} \tag{37}$$

and the velocity and pressure vectors are the same as those just considered, for velocity or pressure cancellation. The two matrices in Eq. (26) are given by

$$\boldsymbol{A}_{v,p} = \begin{bmatrix}\boldsymbol{S}_{\mathrm{rm}}\boldsymbol{Q}_{\mathrm{sv}} \\ \boldsymbol{P}_{1c}\boldsymbol{S}_{\mathrm{sre}}\boldsymbol{Q}_{\mathrm{sv}} + \boldsymbol{P}_{2c}\end{bmatrix}^H \begin{bmatrix}\boldsymbol{S}_{\mathrm{rm}}\boldsymbol{Q}_{\mathrm{sv}} \\ \boldsymbol{P}_{1c}\boldsymbol{S}_{\mathrm{sre}}\boldsymbol{Q}_{\mathrm{sv}} + \boldsymbol{P}_{2c}\end{bmatrix} \tag{38}$$

$$\boldsymbol{b}_{v,p} = \begin{bmatrix}\boldsymbol{S}_{\mathrm{rm}}\boldsymbol{Q}_{\mathrm{sv}} \\ \boldsymbol{P}_{1c}\boldsymbol{S}_{\mathrm{sre}}\boldsymbol{Q}_{\mathrm{sv}} + \boldsymbol{P}_{2c}\end{bmatrix}^H \begin{bmatrix}\boldsymbol{S}_{\mathrm{rm}}\boldsymbol{Q}_{\mathrm{pv}} \\ \boldsymbol{P}_{1c}\boldsymbol{S}_{\mathrm{sre}}\boldsymbol{Q}_{\mathrm{pv}}\end{bmatrix}\boldsymbol{q}_{\mathrm{pf}} \tag{39}$$

IV. System Studied

In general, the fuselage of a commercial aeroplane is composed of a structure of circular rings (frames) and longitudinal stringers on which is wrapped an aluminum skin of thickness varying between 1 and 1.5 mm. The interior of the fuselage is furnished by trim panels fixed on the frames via rubber mounts. The space between the fuselage skin and the trim panels is filled with blankets of insulating material. The main purpose of this cavity treatment is thermal insulation; however, acoustic absorption is also achieved at relatively high frequencies.[22–24] The sketch in Fig. 1 illustrates the main features of the fuselage wall of a commercial aircraft. (The curvature of the frames and fuselage skin is not shown.)

The assumption is made that the trim panel is attached to the frames via active mounts. The control actuator of the active mount could be placed within the space occupied by the frame, as shown in Fig. 1, whereas the velocity sensor should be fixed on the trim panel points connected to the active mount. The control loudspeakers are placed between the trim panel and the blanket of insulating material. They have been placed near the corners of the system so that they couple well with the acoustic modes of the cavity. The control microphones are placed 5 mm from the loudspeakers, as shown in Fig. 1.

Figure 3 shows the geometry of the system that has been modelled. The source panel has been modelled as a flat panel simply supported on the four edges with four stringers equally spaced. The natural frequencies and modes of such a stiffened panel has been derived using a transfer matrix method,[49,50] which has been used in the past by several authors to model the sound transmission through a section of the fuselage at low-intermediate frequency.[36,37] The trim panel has also been modelled as a flat plate, simply supported at the edges parallel to the x axes and free on the edges parallel to the y axes.

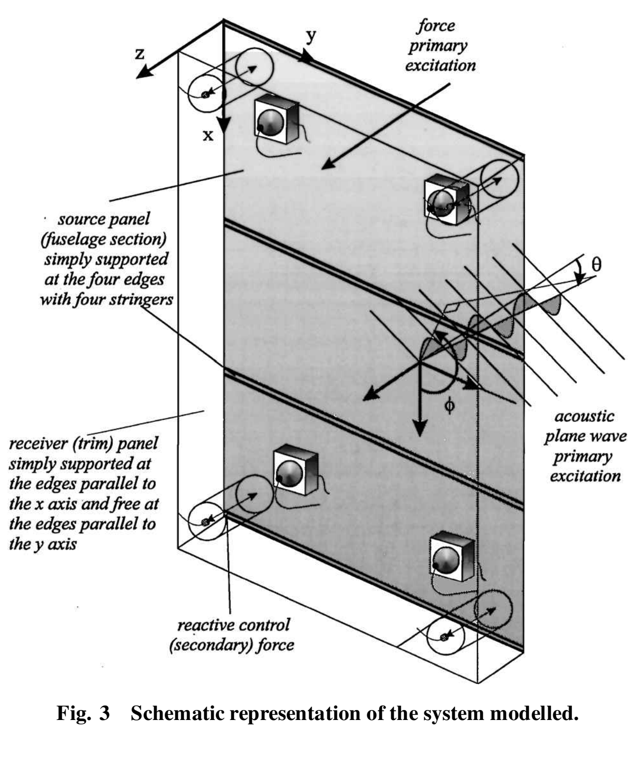

Fig. 3 Schematic representation of the system modelled.

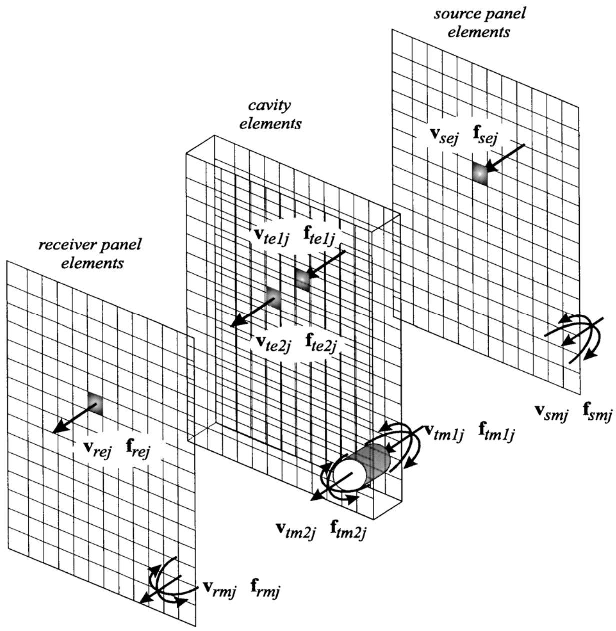

Fig. 4 Mesh of elements for the source and receiver plates and for the acoustic cavity. Source, receiver, and transmitting system velocity and force vector for element and mount junctions.

For both panels the effects of bending waves only have been considered; therefore, at the jth mount junctions the velocity and force vectors, shown in Fig. 4, are defined as

$$\boldsymbol{v}_{\mathrm{mj}} = \begin{Bmatrix} \dot{w}_j \\ \dot{\theta}_{xj} \\ \dot{\theta}_{jy} \end{Bmatrix} \qquad \boldsymbol{f}_{\mathrm{mj}} = \begin{Bmatrix} N_{zj} \\ M_{xj} \\ M_{yj} \end{Bmatrix} \tag{40, 41}$$

whereas the velocity and force vectors at the jth element junction of the two panels account only for the out-of-plane degree-of-freedom as shown in Fig. 4:

$$\boldsymbol{v}_{\mathrm{ej}} = \dot{w}_j \qquad \boldsymbol{f}_{\mathrm{ej}} = N_{zj} \tag{42, 43}$$

The point and transfer mobilities referring to the mount junctions, element junctions, and force excitation positions required in Eqs. (11) and (12) have been calculated using the formulas reported in Appendix C of Ref. 45. The force excitations are harmonic with time dependence $\exp(j\omega t)$. When a plane acoustic wave excites the system, the primary excitation consists of a vector of I point forces $\boldsymbol{q}_p = \{\boldsymbol{N}_{\mathrm{zse1}} \ \cdots \ \boldsymbol{N}_{\mathrm{zse}I}\}^T$ acting on the center of the acoustic I elements of the source panel. If the harmonic incident plane acoustic wave at angles θ and ϕ creates a pressure field on the plate given by

$$p_i = P_o \exp[j(\omega t - k_x x - k_y y)] \tag{44}$$

where P_o is the wave amplitude, $k_x = k\sin\theta\cos\phi$ and $k_y = k\sin\theta\sin\phi$ are the wave numbers in x and y directions and k is the air wave number, then the force at each element junction can be evaluated with the following formula:

$$N_{zj} = 2A_j P_o \exp[-j(k_x x_j + k_y y_j)] \tag{45}$$

where A_j is the area of the jth element and the factor 2 takes into account the pressure doubling at the surface.[26] Equation (44) neglects the fluid loading of the air in the incident field.

The mobility formulas used for the two panels neglect the effects on the source panel related to the fuselage curvature, the cabin pressurization, and external temperature and moisture confined within the fuselage double wall.[51,52] The physical characteristics of the source panel and the weight and stiffness of the receiver panel have been chosen to be similar to those of the fuselage and of the trim panel of a commercial aircraft. The geometry and physical characteristics of the two panels are summarized in Tables 1–3.

The active mounts have each been modelled by a rubber cylinder with two idealized reactive control forces acting at the ends. The dynamics of the actuators have been neglected. In the intermediate frequency range the ring frames vibration is very low when the fuselage section under consideration is excited only acoustically as described in Sec. I. The dynamics of the ring frames have been neglected in the model, and simply supported boundary conditions have been assumed for the fuselage panel along the edges parallel to the x axis. The structural coupling produced by the mounts is provided by coupling the mounts directly to the source and receiver panels, as shown in Fig. 4. The mounts have been placed very close to the edges of the source panel so that the coupling effect is representative of the real system with the frame shown in Fig. 1. The positions of the four mounts are listed in Table 4, whereas the geometry and physical characteristics of the rings of rubber are given by Table 5.

Table 1 Geometry and physical constants for the source panel

Parameter	Value
Dimensions	$l_x = 0.6$ m, $l_y = 0.5$ m
Thickness	$s_1 = 0.0015$ m
Mass density	$\rho_1 = 2796$ kg/m^3
Young's modulus	$E_1 = 7.24 \times 10^{10}$ Pa
Poisson ratio	$\nu_1 = 0.33$
Loss factor	$\eta_1 = 0.02$

Table 2 Geometry and physical constants for the receiver panel

Parameter	Value
Dimensions	$l_x = 0.6$ m, $l_y = 0.5$ m
Thickness	$s_2 = 0.003$ m
Mass density	$\rho_2 = 255$ kg/m^3
Young's modulus	$E_1 = 1 \times 10^9$ Pa
Poisson ratio	$\nu_2 = 0.3$
Loss factor	$\eta_2 = 0.03$

Table 3 Geometry and physical constants for the stringers[50]

Parameter	Value
Frame distances	$b_s = 0.2$ m
Cross-sectional area	$A_s = 1.48 \times 10^{-4}$ m^2
Warping constant of stringer cross section	$C_{\mathrm{ws}} = 4.43 \times 10^{-12}$ m^6
St. Venant torsion cost.	$C = 9.42 \times 10^{-11}$ m^4
Moments of inertia	$I_\eta = 5.08 \times 10^{-8}$ m^4
	$I_{\eta\zeta} = 0$
	$I_\zeta = 3.45 \times 10^{-8}$ m^4
	$J_s = 1.06 \times 10^{-7}$ m^4
Shear center distances	$c_y = 0$, $c_z = 0.02$ m, $s_z = 0.002$ m
Young's modulus	$E_s = 7.24 \times 10^{10}$ Pa
Poisson ratio	$\nu_s = 0.33$
Mass density	$\rho_s = 2796$ kg/m^3

Table 4 Position of the mounts

No.	x, mm	y, mm
1	20	20
2	20	480
3	580	20
4	580	480

Table 5 Geometry and physical constants for the rubber mounts

Parameter	Value
Diameter and height	$\phi = 0.015$, $h = 0.12$ m
Mass density	$\rho_m = 1078$ kg/m^3
Young's modulus	$E_m = 1.5 \times 10^6$ Pa
Poisson ratio	$\nu_m = 0.49$
Loss factor	$\eta_m = 0.05$

The mounts are modelled as distributed systems on which longitudinal and flexural waves can propagate. The point and transfer impedances for each mount required in Eq. (13) have been derived from Appendix B of Ref. 45. The velocity sensors are placed at the connecting points of the mounts with the radiating panel as shown in Fig. 1.

The acoustic cavity confined between the two flexible panels is assumed to be bounded on the four edges by rigid walls and is assumed to be heavily damped. The two panels are divided into a finite number of elements, which vibrate in the direction orthogonal to the area of the element itself and excite the cavity (see Fig. 4). The analytical expression of the point and transfer impedances that relates the pressure, i.e., the normal force, at one cavity element with the velocity imposed at the same (point impedance) or at another cavity element (transfer impedance) can be derived using the modal formulation described in Chap. 10 of Ref. 48. A similar formula is used to evaluate the pressure at one cavity element because of the control loudspeaker excitation or the pressure at the error microphones caused either by the excitations imposed by the cavity elements or by the control loudspeakers. With these equations it is then possible to calculate the relevant impedance terms in Eq. (13).

The geometry and physical characteristics of the cavity are summarized in Table 6, whereas Table 7 gives the positions of the four control loudspeakers and control microphones.

Once the matrices of Eqs. (11–13) have been calculated it is possible to evaluate the total sound power radiation [Eq. (28)] when either only primary or both primary and secondary excitations act on the system. The matrix of radiation resistances in Eq. (28) has been derived, assuming the radiating panel is baffled and neglecting the fluid loading on the plate because of the air in the free field[26]:

$$R = \frac{\omega^2 \rho S^2}{4\pi c}\begin{bmatrix} 1 & \dfrac{\sin(kr_{12})}{kr_{12}} & \cdots & \dfrac{\sin(kr_{1I})}{kr_{1I}} \\ \dfrac{\sin(kr_{21})}{kr_{21}} & 1 & & \\ \cdots & \cdots & \cdots & \cdots \\ \dfrac{\sin(kr_{1I})}{kr_{1I}} & & & 1 \end{bmatrix} \tag{46}$$

where k, ρ, are c the wave number, density, and speed of sound of air in the free field. S is the area of the plate, whereas r_{ij} is the distance from the element i to the element j.

The presence of insulating material in the cavity between the two panels has also been modelled. An equivalent fluid model[53] has been used that takes into account the acoustic wave in the porous part of the insulating material and neglects the effects of the structural waves propagating in the solid structure of the material. The equivalent fluid is assumed to have a complex wave number[53–56]:

$$k_a = k\left[1 + c_7\xi^{c_8} - jc_5\xi^{c_6}\right] \tag{47}$$

Table 6 Geometry and physical constants for the cavity

Parameter	Value
Dimensions	$l_x = 0.6$ m, $l_y = 0.5$ m
Deep	$d = 0.12$ m
Density of air	$\rho_c = 1.19$ kg/m^3
Speed of sound of air	$c_c = 341$ m/s
Modal damping ratio	$\zeta_2 = 0.1$

Table 7 Position of the loudspeakers and microphones

No.	x, mm	y, mm	z (loud), mm	z (mic), mm
1	50	50	72	77
2	50	450	72	77
3	550	50	72	77
4	550	450	72	77

Table 8 Equivalent fluid parameters

Parameter	Value
Dimensions	$l_x = 0.6$ m, $l_y = 0.5$ m
Thickness	$t = 0.72$ m
Flow resistivity	$\sigma = 12{,}000$ Rayls/m
Equivalent fluid constants for fiberglass type materials	$c_1 = 0.070$, $c_2 = -0.632$
	$c_3 = 0.107$, $c_4 = -0.632$
	$c_5 = 0.160$, $c_6 = -0.618$
	$c_7 = 0.109$, $c_8 = -0.618$

and a complex specific impedance

$$Z_a = \rho c\left[1 + c_1\xi^{c_2} - jc_3\xi^{c_4}\right] \tag{48}$$

The constants $c_1, \ldots, c_8$ depend on the type of material in the cavity as described in Ref. 54. Those used here are listed in Table 8. The nondimensional parameter ξ is given by the equation:

$$\xi = f\rho_o/\sigma \tag{49}$$

where σ is the flow resistivity[55] measured in mks Rayls/m.

The point and transfer impedances for the cavity elements have been calculated using the same formulas used for the cavity filled with air, except that the complex wave number, density, and speed of sound for the equivalent fluid have been used. The model also allows the analysis of a cavity partially filled with this porous material, which is possible by considering the space between the two panels occupied by two distinct cavities connected in series. The transmission matrices[57] are derived for each cavity, and then using the four pole theory[58] the impedance matrix for the two cavities in series can been derived.

The validity of the model used here has been verified by comparing the sound reduction index of the double panel calculated using the preceding model with the sound-reduction index calculated with the textbook theory for infinite size double panels.[26] The details of this comparative analysis can be found in Ref. 59.

V. Results with Different Active Control Strategies

The sound transmission through the aircraft panel system described in Sec. IV has been studied for three different cases. In the first two cases the fluid in the cavity has been assumed to be air, and a primary harmonic excitation is assumed to be either a unit force acting at $x_p = 0.15$ m, $x_p = 0.2$ m, or a plane wave of unit amplitude with orientation $\theta_p = 45$ deg and $\phi_p = 135$ deg. In the third case the assumption has been made that the cavity between the two panels is completely filled by porous material with flow resistivity equal to $\sigma = 12{,}000$ Rayls/m. The primary excitation was a plane wave as for the second case. For each case three graphs have been produced; the top plot shows the passive behavior of the double panel system, the center plot shows the when total sound power radiation is minimized using either active mounts and/or control loudspeakers, and the third plot shows when the velocity or the sound pressure is cancelled using either active mounts and/or control loudspeakers.

The top plots of Figs. 5, 6, and 7 show the total sound power radiation by the receiving panel for three different double-panel configurations: 1) when both structure-borne and airborne sound transmission is considered (solid line), 2) when only airborne sound transmission is accounted for (dashed line), and 3) when only structure-borne sound transmission is considered (dash-dotted line). These plots give an overall estimate for the passive sound transmission of the system in the three control cases studied. With reference to the first case, the top plot of Fig. 5 shows that the sound transmission is largely airborne at low frequencies, but both air- and structure-borne components are important at higher frequencies.

Table 9 summarizes the first 10 natural frequencies of the structural modes for the source and receiver panels respectively,[60] whereas Table 10 gives the 12 natural frequencies for the acoustic modes of the cavity that have been used in the simulations. Below the first resonance of the source panel, the sound transmission is quite low, and the double-panel system is controlled by the stiffness of the source panel itself. In the frequency range between 100

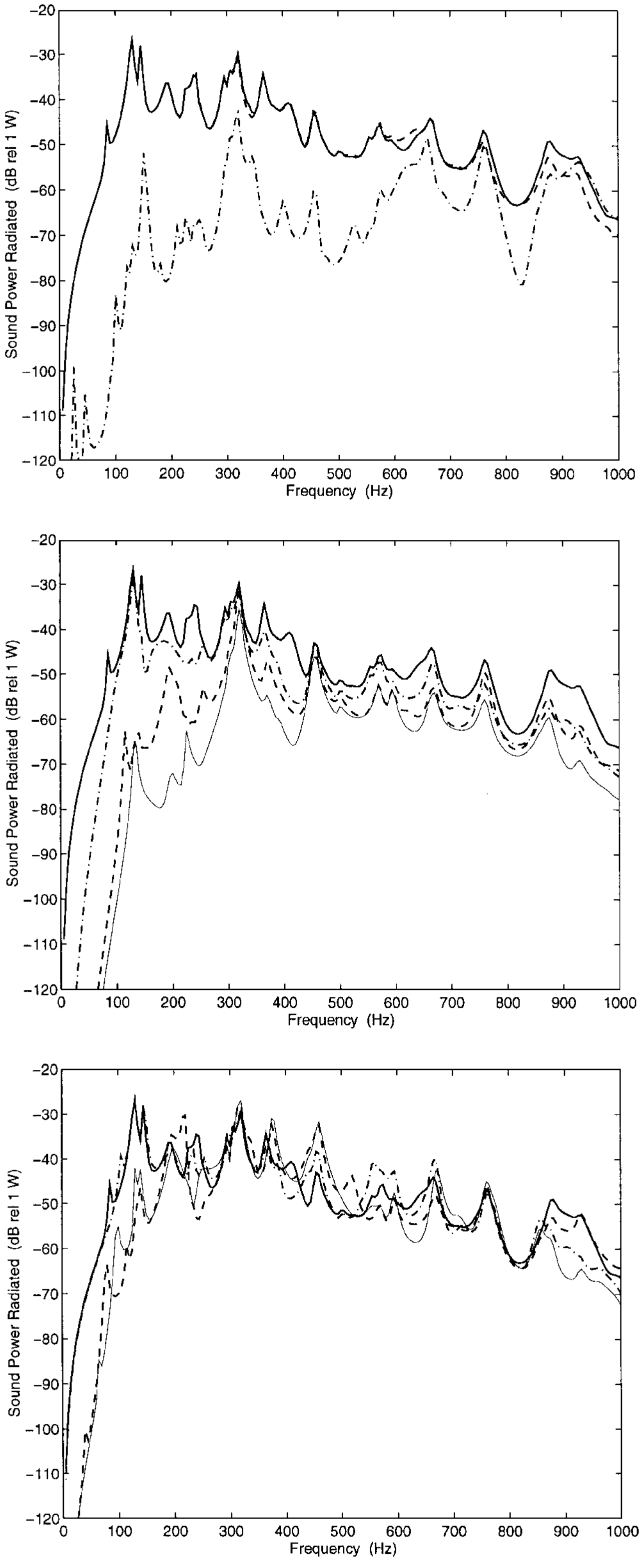

Fig. 5 Case 1: point force primary excitation and gap between the two panels filled by air. Top plot: total sound power radiated when there is both structure-borne and airborne sound transmission (——), only airborne sound transmission (- - -), and only structure-borne sound transmission (- · -). Center plot: total sound power radiated before control (——) and when total sound power radiation is minimized using active mounts (- · -), control loudspeakers (- - -) and both active mounts and control loudspeakers (——). Bottom plot: total sound power radiated before control (——), when active mounts cancel velocities at mount control sensors (- · -), when control loudspeakers cancel sound pressure at control microphones (- - -), and when both active mounts and control loudspeakers cancel velocities and sound pressure (——).

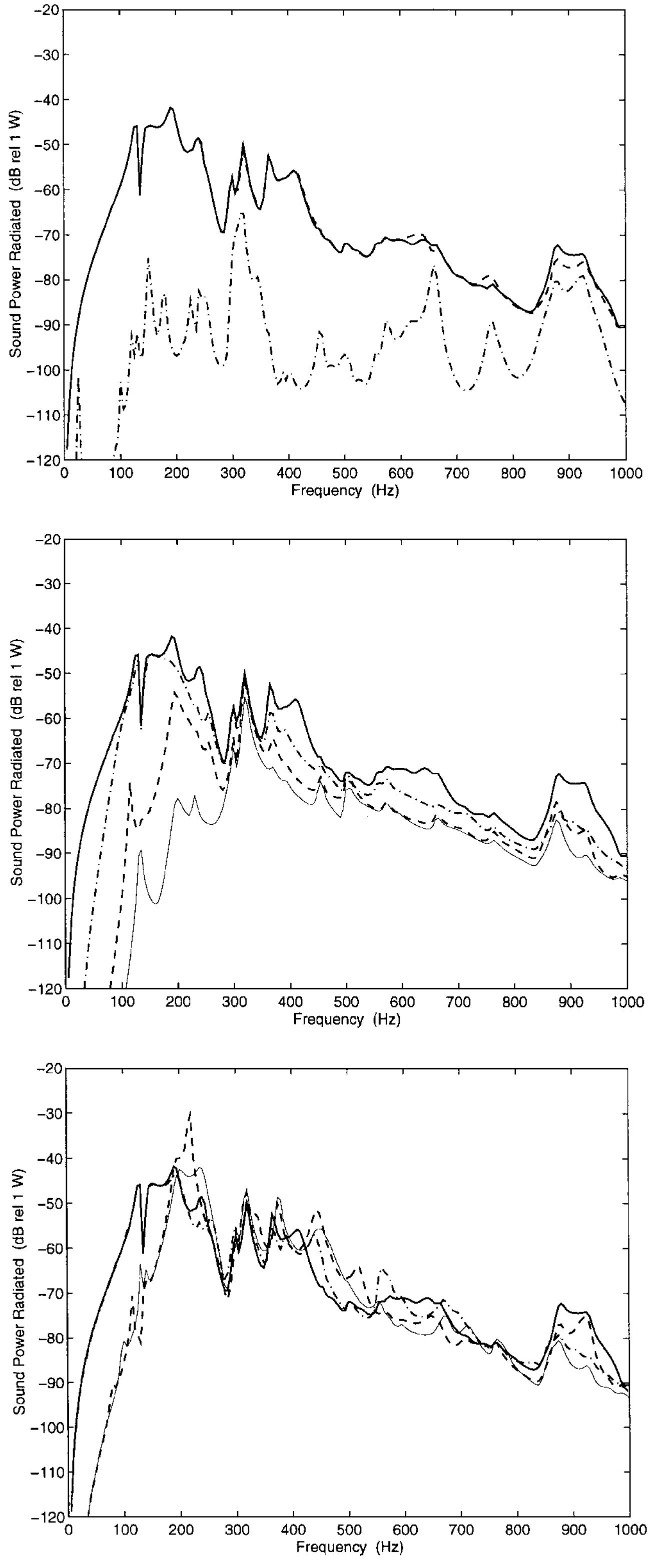

Fig. 6 Case 2: plane acoustic wave primary excitation and gap between the two panels filled by air. Top plot: total sound power radiated when there is both structure-borne and airborne sound transmission (——), only airborne sound transmission (- - -), and only structure-borne sound transmission (- · -). Center plot: total sound power radiated before control (——) and when total sound power radiation is minimized using active mounts (- · -), control loudspeakers (- - -), and both active mounts and control loudspeakers (——). Bottom plot: total sound power radiated before control (——), when active mounts cancel velocities at mount control sensors (- · -), when control loudspeakers cancel sound pressure at control microphones (- - -), and when both active mounts and control loudspeakers cancel velocities and sound pressure (——).

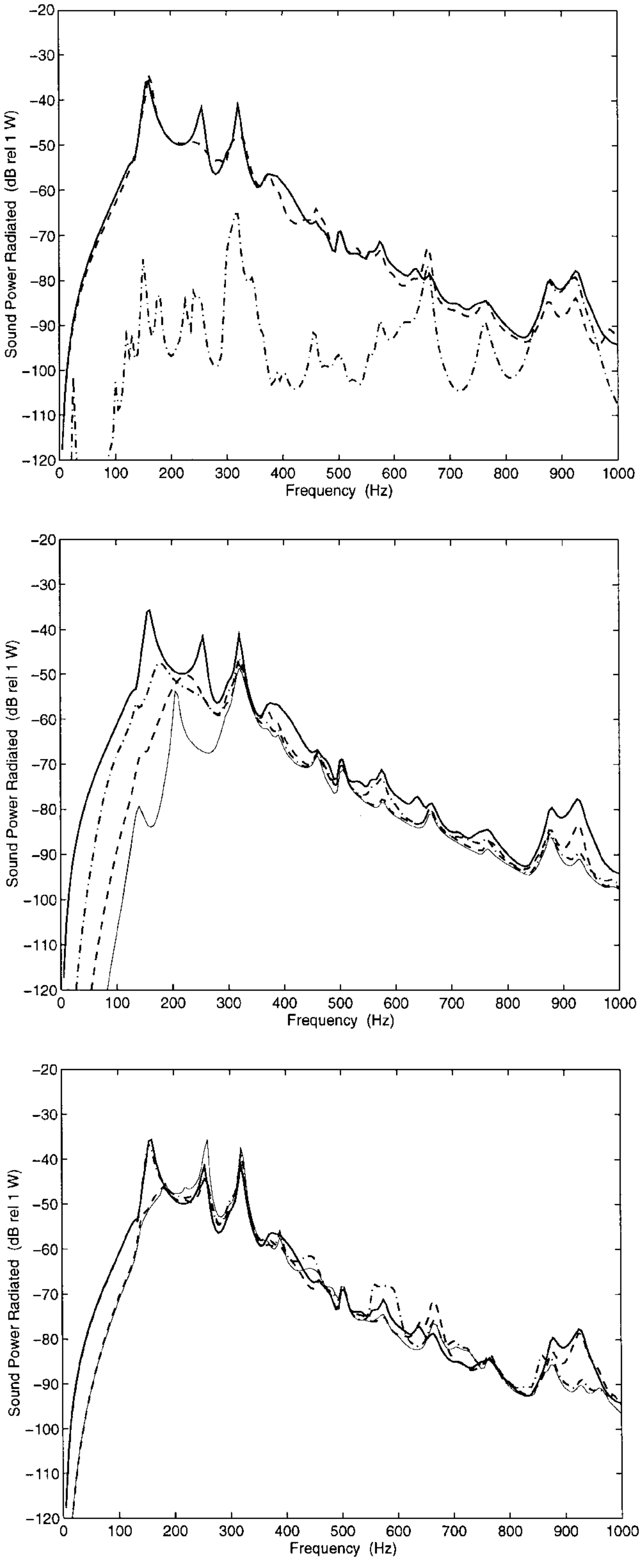

Fig. 7 Case 3: plane acoustic wave primary excitation and gap between the two panels filled by porous material. Top plot: total sound power radiated when there is both structure-borne and airborne sound transmission (——), only airborne sound transmission (- - -), and only structure-borne sound transmission (- · -). Center plot: total sound power radiated before control (——), and when total sound power radiation is minimized using active mounts (- · -), control loudspeakers (- - -), and both active mounts and control loudspeakers (——). Bottom plot: total sound power radiated before control (——), when active mounts cancel velocities at mount control sensors (- · -), when control loudspeakers cancel sound pressure at control microphones (- - -), and when both active mounts and control loudspeakers cancel velocities and sound pressure (——).

Table 9 Natural frequencies of the source and receiver panels[a]

Source panel			Receiver panel		
m	n	$f_{m,n}$, Hz	m	n	$f_{m,n}$, Hz
1	1	131.9	0	1	36.1
2	1	148.8	0′	1	52.7
3	1	177.8	1	1	106.6
1	2	228.8	0	2	144.4
2	2	234.6	0′	2	163.5
3	2	240.5	2	1	204.9
1	3	297.6	1	2	226.7
2	3	298.5	0	3	324.9
3	3	300.4	2	2	331.6
4	1	305.5	0′	3	344.7

[a]0 refers to modes in which both free ends of the panel move in phase and 0′ to those in which the free ends move out of phase.[60]

Table 10 Natural frequencies of the cavity confined between the two panels filled by air

m	n	p	$f_{m,n,p}$, Hz	m	n	p	$f_{m,n,p}$, Hz
0	0	0	0.0	0	2	0	682.0
1	0	0	284.2	1	2	0	738.8
0	1	0	341.0	3	0	0	852.5
1	1	0	443.9	2	2	0	887.8
2	0	0	568.3	3	1	0	918.2
2	1	0	662.8	0	3	0	1023.0

and 250 Hz, the sound transmission is relatively high because it is controlled by the mass-air-mass sound transmission mechanism.[26] In this frequency range the vibration of the two panels is dominated by the resonances of the modes characterized by at least one modal order equal to one that produces a large net volume velocity of the air at both sides of each panel ($f_{s11} = 13.19$, $f_{s21} = 148.8$, $f_{s12} = 228.8$, and $f_{r11} = 106.6$ Hz). The first resonance of the air in the cavity between the two panels is at $f_{c100} = 284.2$ Hz; thus, in the frequency range between 100 and 250 Hz, the air between the two panels acts as a spring that is compressed by the volumetric motion of the two plates. This type of coupling gives rise to a resonant effect, known as the mass-air-mass resonance of double partitions,[26] that strongly couples the two panels. Moreover, the volumetric motion of the receiver panel efficiently radiates sound. The combined effect of mass-air-mass sound transmission mechanism and efficient sound radiation of the receiver panel is the cause of the relatively high level of sound transmission in the frequency band between 100 and 250 Hz. At higher frequencies the acoustic response in the cavity confined between the two panels is also characterized by resonances. Therefore, for frequencies above 250 Hz, the airborne sound transmission is controlled by the coupling of the modes of the two panels with the modes of the cavity confined between them. This results in a reduction of the sound transmission except at about 310 Hz, where the vibration of the receiver panel is controlled by modes with a component equal to one which efficiently radiates sound.

The same type of trend is obtained with an incident plane wave excitation when the cavity is filled by air as can be seen by comparing the top plot of Figs. 5 and 6. When the cavity is entirely filled by porous material (top plot of Fig. 7), the effects of the cavity resonances are smoothed by the added dissipative effect. In agreement with the observations of Grosveld,[24] the sound radiation in the frequency range between 100 and 250 the porous material does not produce any benefit. On the contrary, it tends to slightly increase the sound radiation resonance effects caused by the mass-air-mass sound-transmission mechanism and caused by the efficient sound radiation of the receiver panel.

For all three cases studied the performance of the control systems has been calculated in the frequency range between 0 and 1000 Hz, by considering the total sound power radiation without control and with control using the four control strategies listed in Sec. III. Considering the case where the system is excited by the point force and the cavity is filled by air, the center plot of Fig. 5 shows the reduction in total sound power radiation when using either active mounts or control loudspeakers or a combination of the two when these actuators are driven to minimize total sound power radiation. This plot shows that when the control loudspeakers are used attenuations of about 10 dB in the total sound power radiation can be achieved in the mass-air-mass frequency band (below 250 Hz). Above 250 Hz a relatively low reduction of about 4 dB is obtained instead. The active mount system does not perform well either at low frequencies or at high frequencies. When both active mounts and control loudspeakers are used, reductions in radiated power of about 20 dB are achieved below 250 Hz, whereas at higher frequencies the average reduction is about 6 dB. The bottom plot of Fig. 5 shows the total sound power radiation when the active mounts are driven to cancel the out-of-plane input velocities to the receiver plate or when the control loudspeakers are driven to cancel the acoustic pressure at fixed points of the cavity. The control loudspeakers still produce some control in the mass-air-mass frequency band, whereas no control is achieved at higher frequencies. The active mounts produce very poor results with small amplifications at some frequencies.

Considering the center and bottom plots of Figs. 6 and 7, similar conclusions can be drawn when the system is excited by a plane wave, and the air gap between the two panels is filled with air. However, if the control performance of the loudspeakers at mass-air-mass resonances is considered, one can see that because the loudspeakers are fully immersed in the porous material, the control effectiveness is lower compared with that achieved when the gap between the two panels is filled with air.

The results obtained from these three cases suggest that the control loudspeakers could provide good control in the mass-air-mass frequency band while the active mounts are not able to produce any benefit because the control loudspeakers are acting on the air between the two panels, which, as described before, is working as a spring that couples the volumetric motion of the two panels. Therefore the loudspeakers can be used to pump air in and out of the small cavity in such a way as to reduce the volumetric vibration of the receiver panel. This produces both a reduction of the mass-air-mass sound-transmission mechanism and a reduction of the vibration of the receiver panel controlled by modes that are efficient sound radiators. Alternatively, the active mounts are not able to affect the volumetric vibration of the two panels because they are placed at the four corners of the system. Thus, neither the mass-air-mass sound transmission mechanism nor the vibration of the receiver panel controlled by modes, which are efficient sound radiators, can be controlled by the mount configuration studied here. These results indicate that the control loudspeakers could be usefully integrated with the passive techniques of sound transmission isolation because they are able to produce reductions of the sound transmission at the mass-air-mass frequency band where passive isolation provides poor performance.[24]

A final case has been considered where the double-panel system with the cavity filled with air and excited by a plane wave has been provided with a single control loudspeaker system. Figure 8 shows that the control performance is not as good as with the four loudspeakers (center and bottom plots of Figs. 6), but reductions in the noise transmission are still achieved.

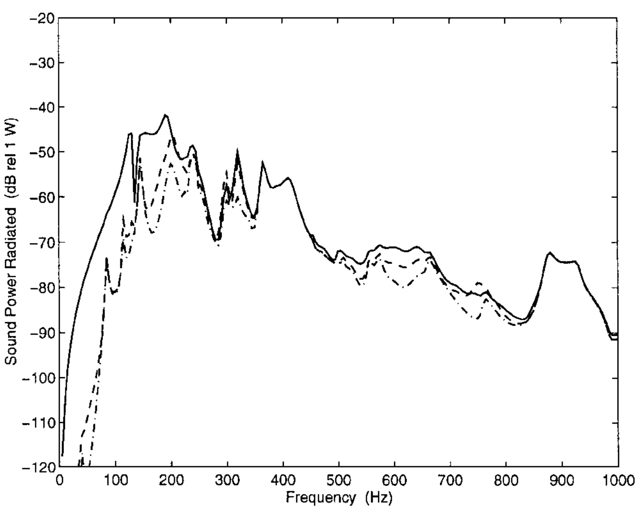

Fig. 8 Total sound power radiated when the double panel with the cavity filled by air is excited by a plane wave. Before control (——). After control when one control loudspeaker is driven to minimize total sound power radiation (– – –) and when one control loudspeaker is driven to cancel sound pressure at the control microphone (– · –).

VI. Conclusions

A theoretical model for sound transmission through a double-panel system has been developed and used to predict the reductions in the total sound power radiated when either control loudspeakers in the partition air gap or active mounts at trim panel attachment points are used. The model accounts for both structure-borne and airborne sound-transmission paths, and the physical and geometrical characteristics of the system studied have been chosen to be similar to those of the fuselage of a civil aircraft. Both point force and acoustic plane wave excitations are considered. The main conclusions drawn from the results of the simulations performed can be listed as follows:

1) The control loudspeakers are able to produce good attenuation of the sound transmission at lower frequencies close to the mass-air-mass resonance frequency band of the double panel.

2) The active mount configuration studied in this paper does not produce significant reductions of the sound transmission except in the case where it is used in combination with the control loudspeakers.

3) For the loudspeaker control system the noise control performance is significantly better if radiated sound power is minimized, rather than cancelling the pressure measured near the loudspeakers.

4) A control system with a single loudspeaker in the partition air gap is estimated to provide some noise control in the mass-air-mass resonance frequency band.

5) When the air gap between the two panels is filled with porous material, the control effectiveness of loudspeakers is slightly reduced.

Acknowledgments

The content of this paper is part of a Brite-Euram project supported by the EC under the Contract BRPR-CT96-0154 DAFNOR, "Distributed Active Foils for Noise Reduction."

References

[1]Mixson, J. S., and Wilby, J. F., "Interior Noise," *Aeroacoustics of Flight Vehicles, Theory and Practice*, edited by H. H. Hubbard, NASA Langley Research Center, Hampton, VA, 1995, Chap. 16.

[2]Mixson, J. S., and Wilby, J. F., "Airplane Interior Noise: A Status Review," AIAA Paper 87-2659, Oct. 1987.

[3]Wilby, J. F., "Noise Transmission into Propeller-Driven Airplanes," *The Shock and Vibration Digest*, Vol. 21, No. 6, 1989, pp. 3–10.

[4]Sulc, J., Hofr, J., and Benda, L., "Exterior Noise on the Fuselage of Light Propeller Driven Aircraft in Flight," *Journal of Sound and Vibration*, Vol. 84, No. 1, 1982, pp. 105–120.

[5]Bhat, W. V., "Flight Test Measurement of Exterior Turbulent Boundary Layer Pressure Fluctuations on Boeing Model 737 Airplane," *Journal of Sound and Vibration*, Vol. 14, No. 4, 1971, pp. 439–457.

[6]Bhat, W. V., and Wilby, J. F., "Interior Noise Radiated by an Airplane Fuselage Subjected to Turbulent Boundary Layer Excitation and Evaluation of Noise Reduction Treatments," *Journal of Sound and Vibration*, Vol. 18, No. 4, 1971, pp. 449–464.

[7]Wilby, J. F., and Gloyna, F. L., "Vibration Measurements of an Airplane Fuselage Structure. I. Turbulent Boundary Layer Excitation," *Journal of Sound and Vibration*, Vol. 23, No. 4, 1972, pp. 443–466.

[8]Wilby, J. F., and Gloyna, F. L., "Vibration Measurements of an Airplane Fuselage Structure. II. Jet Noise Excitation," *Journal of Sound and Vibration*, Vol. 23, No. 4, 1972, pp. 467–486.

[9]Bhat, W. V., "Use of Correlation Technique for Estimating In-Flight Noise Radiated by Wing-Mounted Jet Engines on a Fuselage," *Journal of Sound and Vibration*, Vol. 17, No. 3, 1971, pp. 349–355.

[10]Mixson, J. S., Barton, C. K., and Vaicatis, R., "Investigation of Interior Noise in a Twin-Engine Light Aircraft," *Journal of Aircraft*, Vol. 15, No. 4, 1978, pp. 227–233.

[11]Pope, L. D., Wilby, E. G., and Wilby, J. F., "Propeller Aircraft Interior Noise Model, Part I: Analytical Model," *Journal of Sound and Vibration*, Vol. 118, No. 3, 1987, pp 449–467.

[12]Pope, L. D., Willis, C. M., and Mayes, W. H., "Propeller Aircraft Interior Noise Model, Part II: Scale-Model and Flight-Test Comparison," *Journal of Sound and Vibration*, Vol. 118, No. 3, 1987, pp. 469–493.

[13]Pope, L. D., Rennison, D. C., Willis, C. M., and Mayes, W. H., "Development and Validation of Preliminary Analytical Models for Aircraft Interior Noise Prediction," *Journal of Sound and Vibration*, Vol. 82, No. 4, 1982, pp. 541–575.

[14]Pope, L. D., Wilby, E. G., Willis, C. M., and Mayes, W. H., "Aircraft Interior Noise Models: Sidewall Trim, Stiffened Structures, and Cabin Acoustic with Floor Partition," *Journal of Sound and Vibration*, Vol. 89, No. 3, 1983, pp. 371–417.

[15]Pope, L. D., and Wilby, J. F., "Band-Limited Power Flow into Enclosures. II," *Journal of the Acoustical Society of America*, Vol. 67, No. 3, 1980, pp. 823–826.

[16]Graham, W. R., "Boundary Layer Induced Noise in Aircraft, Part I: The Flat Plate Model," *Journal of Sound and Vibration*, Vol. 192, No. 1, 1996, pp. 101–120.

[17]Graham, W. R., "Boundary Layer Induced Noise in Aircraft, Part II: The Trimmed Flat Plate Model," *Journal of Sound and Vibration*, Vol. 192, No. 1, 1996, pp. 121–138.

[18]Unruh, J. F., "Structure-Borne Noise Control for Propeller Aircraft," *Journal of Aircraft*, Vol. 17, No. 2, 1988, pp. 752–757.

[19]Unruh, J. F., "Installation Effects on Propeller Wake/Vortex-Induced Structure-Borne Noise Transmissions," *Journal of Aircraft*, Vol. 27, No. 5, 1989, pp. 444–448.

[20]Vaicatis, R., "Noise Transmission into a Light Aircraft," *Journal of Aircraft*, Vol. 17, No. 2, 1980, pp. 81–86.

[21]Barton, C. K., and Mixson, J. S., "Noise Transmission and Control for a Light Twin-Engine Aircraft," *Journal of Aircraft*, Vol. 18, No. 7, 1981, pp. 570–575.

[22]Heitman, K. E., and Mixson, J. S., "Laboratory Study of Cabin Acoustic Treatments Installed in an Aircraft Fuselage," *Journal of Aircraft*, Vol. 23, No. 1, 1986, pp. 32–38.

[23]Mixson, J. S., Roussos, L. A., Barton, C. K., Vaicaitis, R., and Slazak, M., "Laboratory Study of Add-On Treatments for Interior Noise Control in Light Aircraft," *Journal of Aircraft*, Vol. 20, No. 6, 1983, pp. 516– 522.

[24]Grosveld, F. W., "Field-Incidence Noise Transmission Loss of General Aviation Aircraft Double-Wall Configurations," *Journal of Aircraft*, Vol. 22, No. 2, 1985, pp. 117–123.

[25]Desmet, W., and Sas, P., "Sound Transmission of Finite Double-Panel Partitions with Sound Absorbing Material and Panel Stiffeners," CEAS/AIAA Paper 95-043, June 1995.

[26]Fahy, F. J., *Sound and Structural Vibration*, Academic International Press, London, 1994, p. 169.

[27]Carneal, J., and Fuller, C. R., "Active Structural Acoustic Control of Noise Transmission Through Double-Panel Systems," *AIAA Journal*, Vol. 33, No. 4, 1995, pp. 618–623.

[28]Sas, P., Bao, C., Augusztinovicz, F., and Desmet, W., "Active Control of Sound Transmission Through a Double Panel Partition," *Journal of Sound and Vibration*, Vol. 180, No. 4, 1995, pp. 609–625.

[29]Bao, C., and Pan, J., "Experimental Study of Different Approaches for Active Control of Sound Transmission Through Double Walls," *Journal of the Acoustical Society of America*, Vol. 102, No. 3, 1997, pp. 1664–1670.

[30]Grosveld, F. W., and Shepherd, K. P., "Active Sound Attenuation Across a Double Wall Structure," *Journal of Aircraft*, Vol. 31, No. 1, 1994, pp. 223–227.

[31]Thomas, D. R., Nelson, P. A., Pinnington, R. J., and Elliott, S. J., "Active Control of Sound Transmission Through Stiff Lightweight Composite Fuselage Constructions," *Proceedings of 14th AIAA Aeroacoustics Conference II*, AIAA, Washington, DC, 1992, pp. 552–560.

[32]Simpson, M. A., Luong, T. M., Fuller, C. R., and Jones, J. D., "Full-Scale Demonstration Tests of Cabin Noise Reduction Using Active Vibration Control," *Journal of Aircraft*, Vol. 28, No. 3, 1990, pp. 208–215.

[33]Rosen, A., and Singer, J., "Vibrations of Axially-Loaded Stiffened Cylindrical Shells," *Journal of Sound and Vibration*, Vol. 34, No. 3, 1974, pp. 357–378.

[34]Mercadal, M., and Flotow, A. H., "On the Importance of Representative Structural Models in Turboprop Acoustics," *Journal of Sound and Vibration*, Vol. 188, No. 5, 1995, pp. 753–759.

[35]Koval, L. R., "On Sound Transmission into a Stiffened Cylindrical Shell with Rings and Stringers Treated as Discrete Elements," *Journal of Sound and Vibration*, Vol. 71, No. 4, 1980, pp. 511–521.

[36]Vaicatis, R., Grosveld, F. W., and Mixson, J. S., "Noise Transmission Through Aircraft Panels," *Journal of Aircraft*, Vol. 22, No. 4, 1985, pp. 303–310.

[37]Vaicatis, R., and Slazak, M., "Noise Transmission Through Stiffened Panels," *Journal of Sound and Vibration*, Vol. 70, No. 3, 1980, pp. 413–426.

[38]Chang, M. T., and Vaicatis, R., "Noise Transmission into Semicylindrical Enclosures Through Discretely Stiffened Curved Panels," *Journal of Sound and Vibration*, Vol. 85, No. 1, 1982, pp. 71–83.

[39]Beranek, L. L., "Sound Transmission Through Multiple Structures Containing Flexible Blankets," *Journal of the Acoustical Society of America*, Vol. 21, No. 4, 1949, pp. 419–428.

[40]London, A., "Transmission of Reverberant Sound Through Double Walls," *Journal of the Acoustical Society of America*, Vol. 22, No. 2, 1950, pp. 270–279.

[41]Mulholland, K. A., Price, A. J., and Parbrook, H. D., "Transmission Loss of Multiple Panels in a Random Incidence Field," *Journal of the Acoustical Society of America*, Vol. 43, No. 6, 1968, pp. 1432–1435.

[42]White, P. H., and Powell, A., "Transmission of Random Sound and Vibration Through a Rectangular Double Wall," *Journal of the Acoustical Society of America*, Vol. 40, No. 4, 1966, pp. 821–832.

[43]Mulholland, K. A., Parbrook, H. D., and Cummings, A., "The Transmission Loss of a Double Panel," *Journal of Sound and Vibration*, Vol. 6, No. 3, 1967, pp. 324–334.

[44]Cummings, A., and Mulholland, K. A., "The Transmission Loss of Finite Sized Double Panels in a Random Incidence Sound Field," *Journal of Sound and Vibration*, Vol. 8, No. 1, 1968, pp. 126–133.

[45]Gardonio, P., Elliott, S. J., and Pinnington, S. J., "Active Isolation of Structural Vibration on a Multiple-Degree-of-Freedom System, Part I: The Dynamics of the System," *Journal of Sound and Vibration*, Vol. 207, No. 2, 1997, pp. 61–93.

[46]O'Hara, G. J., "Mechanical Impedance and Mobility Concepts," *Journal of the Acoustical Society of America*, Vol. 41, No. 5, 1967, pp. 1180–1184.

[47]Johnson, M. E., and Elliott, S. J., "Active Control of Sound Radiation Using Volume Velocity Cancellation," *Journal of the Acoustical Society of America*, Vol. 98, No. 4, 1995, pp. 2174–2186.

[48]Nelson, P. A., and Elliott, S. J., *Active Control of Sound*, Academic International Press, London, 1992, p. 382.

[49]Lin, Y. K., *Probabilistic Theory of Structural Dynamics*, Mc Graw–Hill, New York, 1967.

[50]Lin, Y. K., and Donaldson, B. K., "A Brief Survey of Transfer Matrix Techniques with Special Reference to the Analysis of Aircraft Panels," *Journal of Sound and Vibration*, Vol. 10, No. 1, 1969, pp. 103–143.

[51]Koval, L. R., "Effect of Air Flow, Panel Curvature, and Internal Pressurization on Field-Incidence Transmission Loss," *Journal of the Acoustical Society of America*, Vol. 59, No. 6, 1976, pp. 1379–1385.

[52]Lyrintzis, C. S., and Bofilios, D. A., "Hygrothermal Effects on Structure-Borne Noise Transmission of Stiffened Laminated Composite Plates," *Journal of Aircraft*, Vol. 27, No. 8, 1990, pp. 722–730.

[53]Delany, M. E., and Bazley, E. N., "Acoustical Properties of Fibrous Absorbent Materials," *Applied Acoustics*, Vol. 3, No. 3, 1970, pp. 105–116.

[54]Miki, Y., "Acoustical Properties of Porous Materials—Modifications of Delany-Bazley Models," *Journal of the Acoustical Society of Japan*, Vol. 11, No. 1, 1990, pp. 19–24.

[55]Bies, D. A., and Hansen, C. H., "Flow Resistance Information for Acoustical Design," *Applied Acoustics*, Vol. 13, No. 5, 1980, pp. 357–391.

[56]Wilson, R., and Cummings, A., "Radiation Damping in Plates Induced by Porous Media," *Proceedings of the Institute of Acoustics*, Vol. 18, Pt. 3, St. Albans, Herts, England, UK, 1996, pp. 49–56.

[57]Rubin, S., "Mechanical Immittance- and Transmission-Matrix Concepts," *Journal of the Acoustical Society of America*, Vol. 41, No. 5, 1967, pp. 1171–1179.

[58]Snowdon, J. C., "Mechanical Four-Pole Parameters and Their Application," *Journal of Sound and Vibration*, Vol. 15, No. 3, 1970, pp. 307–323.

[59]Gardonio, P., and Elliott, S. J., "Active Control of Structure-Borne and Air-Borne Sound Transmission Through a Double Panel," AIAA Paper 98-2353, June 1998.

[60]Warburton, G. B., "The Vibration of Rectangular Plates," *Proceedings of the Institute of Mechanical Engineering*, Vol. 168, 1951, pp. 371–381.